ARTICLE

LILRB4 ITIMs mediate the T cell suppression and infiltration of acute myeloid leukemia cells

Zunling Li[1,2], Mi Deng[2], Fangfang Huang[2,3], Changzhu Jin[1], Shuang Sun[1], Heyu Chen[2], Xiaoye Liu[2], Licai He[2,4], Ali H. Sadek[2] and Cheng Cheng Zhang[2]

We recently demonstrated that leukocyte Ig-like receptor 4 (LILRB4) expressed by monocytic acute myeloid leukemia (AML) cells mediates T-cell inhibition and leukemia cell infiltration via its intracellular domain. The cytoplasmic domain of LILRB4 contains three immunoreceptor tyrosine-based inhibitory motifs (ITIMs); the tyrosines at positions 360, 412, and 442 are phosphorylation sites. Here, we analyzed how the ITIMs of LILRB4 in AML cells mediate its function. Our in vitro and in vivo data show that Y_{412} and Y_{442}, but not Y_{360}, of LILRB4 are required for T-cell inhibition, and all three ITIMs are needed for leukemia cell infiltration. We constructed chimeric proteins containing the extracellular domain of LILRB4 and the intracellular domain of LILRB1 and vice versa. The intracellular domain of LILRB4, but not that of LILRB1, mediates T-cell suppression and AML cell migration. Our studies thus defined the unique signaling roles of LILRB4 ITIMs in AML cells.

Keywords: LILRB4; ITIM motifs; AML; T cell suppression; infiltration

Cellular & Molecular Immunology (2020) 17:272–282; https://doi.org/10.1038/s41423-019-0321-2

INTRODUCTION

The leukocyte Ig-like receptor subfamily B (LILRB) proteins are a group of type I transmembrane glycoproteins with extracellular Ig-like domains that bind ligands and intracellular immunoreceptor tyrosine-based inhibitory motifs (ITIMs) that can recruit the tyrosine phosphatases SHP-1 and SHP-2, and/or the inositol phosphatase SHIP.[1–6] LILRBs are expressed on various types of immune and non-immune cells.[1] Because of the negative roles of phosphatases in immune activation, LILRBs are considered to be immune checkpoint factors.[7]

LILRBs are also expressed by tumor cells, notably hematopoietic cancer cells.[1,8,9] We have shown that several LILRBs and a related ITIM receptor, LAIR1, support AML development.[10–13] Consistently, other laboratories have demonstrated that LILRB4, LILRB1, and LAIR1 support tumor development,[14–16] and several LILRBs have been suggested to be AML target candidates.[17]

LILRB4 (also known as ILT3, LIR5, and CD85K) is expressed specifically on normal monocytic cells (monocytes, macrophages, and some dendritic cells)[13,18] and to a lesser extent on plasmablasts[19] but not on hematopoietic progenitor or stem cells.[1,12,13,20,21] LILRB4 is a marker for monocytic AML, and it is expressed at significantly higher levels on monocytic AML cells than on normal hematopoietic cells.[12,13,21,22] It is noteworthy that LILRB4 is primate-specific. The expression pattern and ligand of the mouse orthologue of LILRB4—gp49B1—are different from those of LILRB4.[1,12] Therefore, the *gp49B1* knockout mouse model may not be appropriate for use in experiments seeking to elucidate the biological significance of LILRB4.

We discovered that LILRB4 supports tumor growth by facilitating leukemia cell infiltration into tissues and by suppressing T-cell activity through the apolipoprotein E (ApoE)/LILRB4/tyrosine-protein phosphatase nonreceptor type 11 (SHP-2)/nuclear factor kappa-B (NFκB)/urokinase receptor (uPAR)/arginase-1 (ARG1) axis in AML cells.[12,22] Extracellular ApoE can activate LILRB4 on monocytic AML cells, and the intracellular domain of LILRB4 is required to mediate the signaling and activities.[12] The activated LILRB4 subsequently recruits SHP-2 and upregulates NFκB.[12,22,23] Downstream effectors of NFκB in AML cells, including ARG1 and uPAR, lead to inhibition of T-cell proliferation and promotion of tissue infiltration.[12] In addition, we also developed anti-LILRB4 CAR-T cells that efficiently inhibited AML development in vitro and in vivo.[12,13] LILRB4 thus represents an attractive target for treating monocytic AML. Our work suggests that LILRBs have dual roles in tumor biology: as immune checkpoint molecules and as tumor-sustaining factors.[1]

How the intracellular domain of LILRB4 regulates signaling is an unresolved question. ITIMs are thought to be the only signaling motif in LILRBs. LILRB4 contains three ITIMs, with tyrosines at positions 360, 412, and 442 as phosphorylation sites.[18,24,25] The functions of LILRB4 ITIMs in malignant cells remain unknown. To define the roles of the individual ITIMs of LILRB4 in mediating LILRB4 functions in cancer cells, we individually mutated each of these tyrosines to phenylalanines to disrupt ITIM domain functions, swapped the domains of LILRB1 and LILRB4, and used functional assays to analyze the effects.

[1]Basic Medicine School, Binzhou Medical University, Yantai, Shandong 264003, China; [2]Department of Physiology, University of Texas Southwestern Medical Center, 5323 Harry Hines Boulevard, Dallas, TX 75390, USA; [3]Department of Hematology, Zhongshan Hospital, Xiamen University, Xiamen, Fujian 361000, China and [4]Key Laboratory of Laboratory Medicine, Ministry of Education, School of Laboratory Medical and Life Science, Wenzhou Medical University, Wenzhou 325035, China
Correspondence: Cheng Cheng Zhang (Alec.Zhang@UTSouthwestern.edu)
These authors contributed equally: Zunling Li, Mi Deng

Received: 30 May 2019 Accepted: 14 October 2019
Published online: 7 November 2019

RESULTS

Tyrosines at positions 412 and 442 but not 360 in ITIMs are required for the T-cell inhibition mediated by LILRB4 in leukemia cells

The intracellular domain of LILRB4 contains three ITIMs centered on Y_{360} (VTYAKV), Y_{412} (VTYARL), and Y_{442} (SVYATL).[18,24,25] To identify the tyrosine residues that mediate T-cell suppression and AML cell infiltration, we mutated each tyrosine to phenylalanine and introduced a version of LILRB4 with single, double, or triple mutations into *lilrb4*-KO THP-1 monocytic AML cells by lentivirus-mediated transduction (Fig. 1a). We cocultured wild-type control and engineered THP-1 cells with primary human T cells without cell-cell contact in a 96-well permeable support system. The dilution of CFSE represents T-cell proliferation (Supplementary Figs. S1A and B). Consistent with our previous observations,[12] the *lilrb4*-WT but not the *lilrb4*-KO THP-1 cells inhibited T-cell proliferation, and the KO phenotype was reversed by the expression of *lilrb4* in *lilrb4*-KO THP-1 cells (*lilrb4*-Res cells) (Fig. 1b, c, Supplementary Figs. S1C and D). Interestingly, in cocultures with *lilrb4*-KO cells in which the $Y_{360}F$ mutant was expressed, T-cell proliferation was inhibited to the same extent as was observed upon expression of WT LILRB4. In contrast, expression of $Y_{412}F$ or $Y_{442}F$ did not restore wild-type levels of inhibition of T-cell proliferation (Fig. 1b, c, Supplementary Figs. S1 B, C and D). The expression of the double mutants or the triple mutant in *lilrb4*-KO cells did not restore T-cell inhibition (Fig. 1b, c, Supplementary Figs. S1B, C and D). Similar results were obtained when LILRB4 constructs were expressed in MV4-11 *lilrb4*-KO cells (Fig. 1d–e, Supplementary Fig. S2). These results indicate that Y_{412} and Y_{442}, but not Y_{360}, are required for LILRB4-mediated T-cell inhibition by monocytic AML cells.

Next, we used a humanized mouse xenograft model to determine the function of ITIMs in immune checkpoint blockade in vivo. Immune compromised NOD-scid IL2Rγ-knockout (NSG) mice were humanized by injection of human PBMCs. THP-1 cells expressing *lilrb4* constructs were subcutaneously transplanted into the humanized mice, and the tumor development and T-cell numbers were monitored. Tumors developed significantly faster in groups transplanted with *lilrb4*-WT, *lilrb4*-Res, and *lilrb4*-$Y_{360}F$ cells than in groups transplanted with *lilrb4*-KO, *lilrb4*-$Y_{412}F$, and *lilrb4*-$Y_{442}F$ cells (Fig. 2a–c). Moreover, human $CD3^+$ T-cell percentages in peripheral blood were significantly higher in the *lilrb4*-KO, *lilrb4*-$Y_{412}F$, and *lilrb4*-$Y_{442}F$ groups than in the *lilrb4*-WT, *lilrb4*-Res, and *lilrb4*-$Y_{360}F$ groups (Fig. 2d). Thus, in vitro and in vivo data indicate that T-cell inhibition is mediated by the two distal ITIMs (Y_{412} and Y_{442}) but not the proximal ITIM (Y_{360}) of LILRB4 in AML cells.

All three ITIMs of LILRB4 influence leukemia cell infiltration

Patients with monocytic AML are more likely to have extramedullary infiltration than patients with other leukemias,[26,27] and LILRB4-mediated signaling supports the infiltration activity of monocytic AML cells.[12] To determine which ITIMs mediate this tissue infiltration ability, we employed a *trans*-endothelial migration assay to compare the abilities of LILRB4 ITIM mutants to migrate through endothelial cells. A much higher number of THP-1 cells that expressed *lilrb4*-WT migrated through the endothelial cells than did THP-1 cells that expressed *lilrb4*-KO; expression of *lilrb4* in the *lilrb4*-KO cells (*lilrb4*-Res) rescued the defective migration of *lilrb4*-KO cells (Fig. 3a, b), consistent with our previous report.[12] Interestingly, the cells with single, double, or triple mutations of the tyrosines in the ITIM domains all demonstrated less *trans*-endothelial migration than was observed for cells that expressed wild-type LILRB4 (Fig. 3a, b, Supplementary Fig. S3).

To validate the in vitro results, we analyzed the short-term infiltration abilities of *lilrb4*-KO MV4-11 cells that stably expressed various LILRB4 mutants in vivo. The ratio of GFP^+ cells to peripheral blood represented the infiltration abilities, and the GFP^+ cell percentages in peripheral blood, bone marrow, spleen and liver are shown in Supplementary Figs. S4 and S5. The *lilrb4*-KO cells injected intravenously into NSG mice had significantly less infiltration into the bone marrow, spleen, and liver than *lilrb4*-WT cells. Expression of *lilrb4* in the *lilrb4*-KO cells significantly promoted the infiltration of the cells into these organs (Fig. 3c–e). In contrast, leukemia cell infiltration into the bone marrow, spleen, and liver was significantly reduced when any of the ITIMs were mutated (Fig. 3c–e). Therefore, we conclude that each ITIM of LILRB4 regulates the AML cell infiltration capacity.

Y412 and Y442, but not Y360, recruit SHP-2 to activate downstream signaling

The intracellular domain of activated LILRB4 recruits SHP-2, which activates NFκB.[12] NFκB regulates downstream effectors, including uPAR[28] and ARG1,[29] to inhibit T-cell proliferation and promote the infiltration of AML cells into tissues.[12,22] To identify the ITIMs responsible for SHP-2 recruitment, we first used immunohistochemistry to evaluate the levels of the signaling molecules downstream of LILRB4 in tumor sections from humanized NSG mice transplanted with *lilrb4*-KO THP-1 cells expressing the LILRB4 constructs. The staining of phospho-SHP-2 (Y_{580}), phospho-P65 (S_{536}), and ARG1 was significantly more intense in samples from the *lilrb4*-WT, *lilrb4*-Res, and *lilrb4*-$Y_{360}F$ groups than in samples from the *lilrb4*-KO and *lilrb4*-$Y_{412}F$ groups (Fig. 4). The analysis was not performed for the *lilrb4*-$Y_{442}F$ group because no tumors formed in these mice.

Coimmunoprecipitation (co-IP) was conducted to validate the recruitment. SHP-2 was recruited to LILRB4 in *lilrb4*-WT but not KO cells, and forced expression of *lilrb4* in the *lilrb4*-KO cells led to re-recruitment of SHP-2 (Supplementary Fig. S6A). SHP-2 could be recruited to $Y_{360}F$, $Y_{412}F$, $Y_{442}F$, $Y_{360-412}F$, and $Y_{360-442}F$ mutants, but not to $Y_{412-442}F$ or $Y_{360-412-442}F$ mutants (Supplementary Fig. S6A), suggesting that Y_{412} and Y_{442} of LILRB4 contribute to SHP-2 recruitment.

Western blotting and flow cytometry were used to detect downstream molecules, including phospho-SHP-2, phospho-P65, ARG1, and uPAR, in stably engineered THP-1 cells. The results showed that the levels of phosphorylation of SHP-2 on the Y_{580} residue, P65 on the S_{536} residue, ARG1 and uPAR were decreased upon *lilrb4* knockout, and their levels could be rescued when wild-type *lilrb4* was expressed in the *lilrb4*-KO cells (Fig. 5a–d). The levels of phospho-SHP-2 (Y_{580}), phospho-P65 (S_{536}), ARG1, and uPAR were similar in *lilrb4*-$Y_{360}F$ cells and *lilrb4*-WT cells; however, their levels were decreased in *lilrb4*-$Y_{412}F$ and *lilrb4*-$Y_{442}F$ cells (Fig. 5). These results suggest that Y_{412} and Y_{442}, but not Y_{360}, are involved in the downstream signaling mediated by LILRB4 in AML cells.

Furthermore, we found that all three ITIMs of LILRB4 were involved in the regulation of the extramedullary infiltration of AML cells (Fig. 3). The F-actin level was significantly decreased in *lilrb4*-KO cells compared with that in the *lilrb4*-WT group and was significantly restored in *lilrb4*-KO cells ectopically expressing *lilrb4* (Supplementary Fig. S6B). F-actin was significantly reduced in the $Y_{360}F$, $Y_{412}F$, and $Y_{442}F$ mutants (Supplementary Fig. S6B), indicating that F-actin is regulated by the LILRB4 signaling that promotes the infiltration of AML cells.

The intracellular domain of LILRB4, but not that of LILRB1, mediates the T-cell suppression and infiltration of AML cells

The LILRB family contains five members with highly conservative ITIMs in their intracellular domains.[1] Whether the intracellular domains of other LILRBs can mediate the same signaling and function of LILRB4 is unknown. We engineered vectors for the expression of chimeric proteins with the extracellular domain (ECD) of LILRB4 or LILRB1 and the intracellular domain (ID) of the other and stably expressed these proteins in *lilrb4*-KO and *lilrb1*-KO cells (Fig. 6a, b). LILRB1 was chosen for domain swapping for the following reasons. First, LILRB1 and LILRB4 have similar

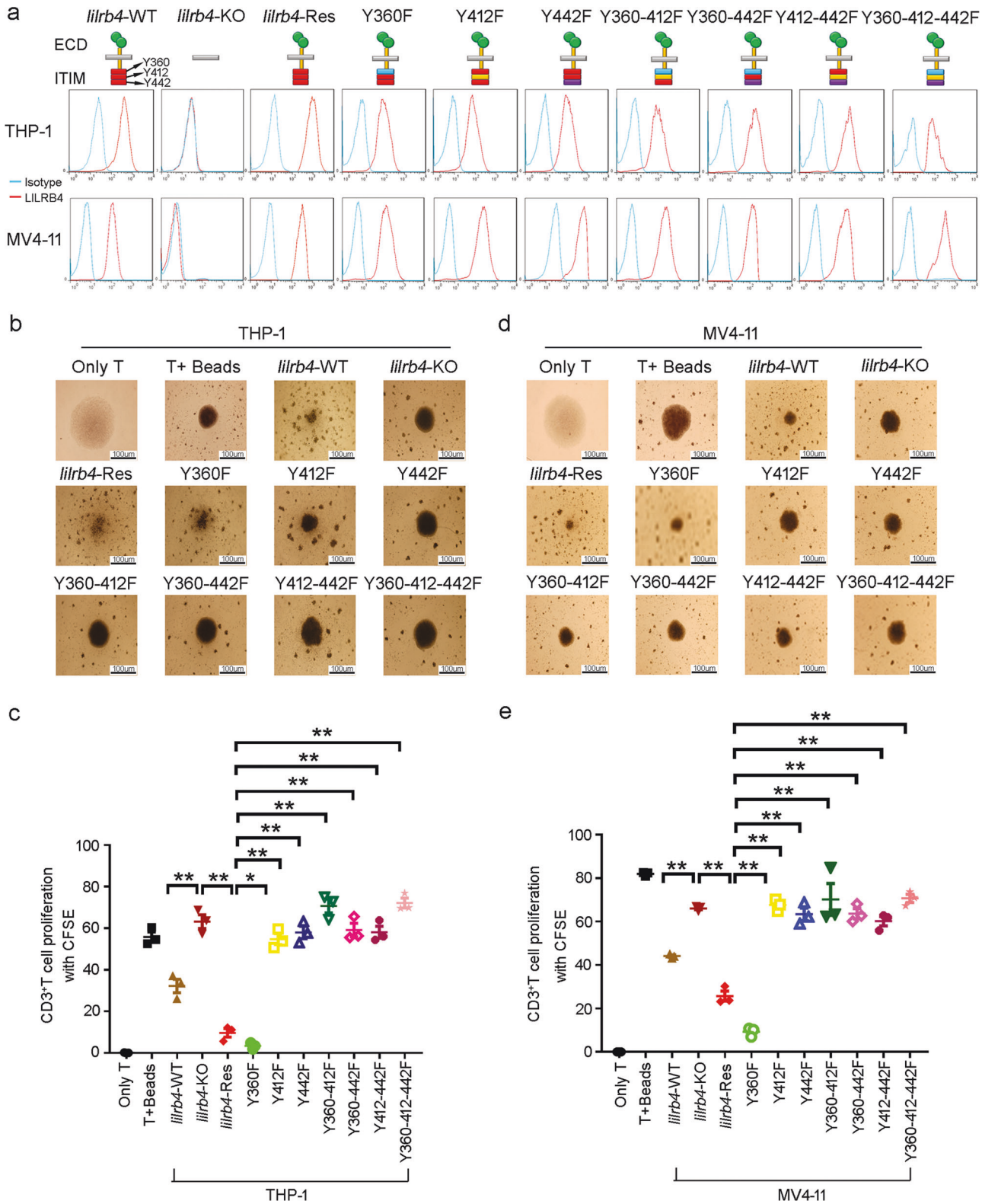

Fig. 1 Y_{412} and Y_{442}, but not Y_{360}, of LILRB4 are required for AML-mediated T-cell inhibition in vitro. **a** Single, double, and triple mutants of phosphorylation sites (shown schematically above the FACS traces confirming expression) were constructed and expressed in THP-1 cells and MV4-11 cells in which *lilrb4* was knocked out. In the construct schematics, wild-type ITIMs are indicated by red. **b**–**e** $CD3^+$ T cells from a healthy donor labeled with CFSE were placed into the lower chamber with anti-CD3/CD28-coated beads and rhIL-2, and irradiated AML cells were placed into the upper chamber. The AML cells were (**b**, **c**) THP-1 cells expressing the indicated constructs and (**d**, **e**) MV4-11 cells expressing the indicated constructs. **b**, **d** Cells were photographed after 5 days (scale bar: 100 μm). **c**, **e** Cells were analyzed by flow cytometry. The dilution of CFSE corresponds to T-cell proliferation. Representative data from three independent experiments are presented ($n = 3$, means ± s.e.m.). $^*p < 0.05$, $^{**}p < 0.01$

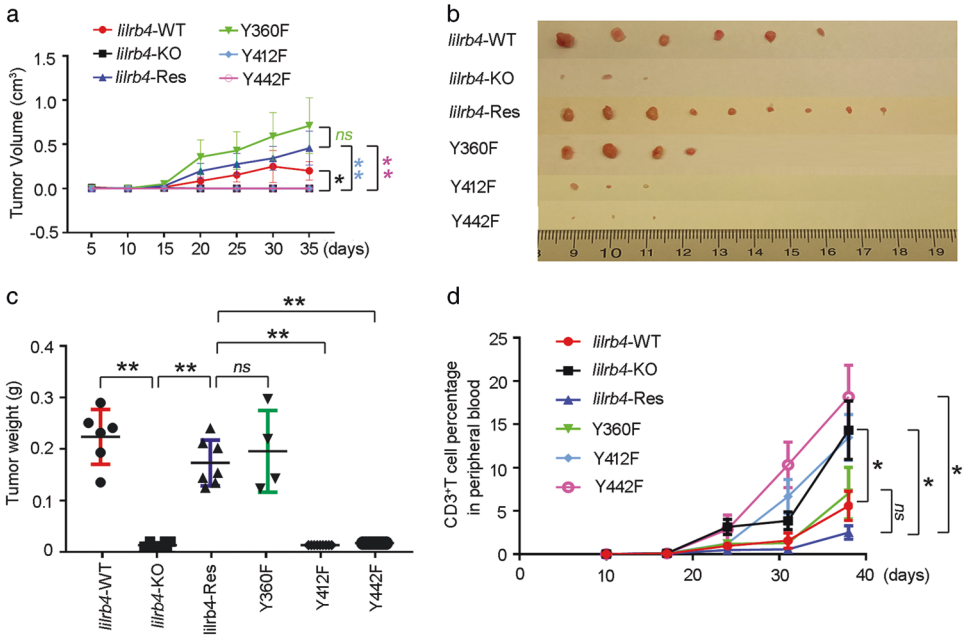

Fig. 2 Y_{412} and Y_{442}, but not Y_{360}, of LILRB4 are required for T-cell inhibition in human T cell-reconstituted immune-deficient mice. Humanized NSG mice were transplanted with 1×10^7 *lilrb4*-WT, *lilrb4*-KO, *lilrb4*-Res, *lilrb4*-Y_{360}F, *lilrb4*-Y_{412}F, or *lilrb4*-Y_{442}F THP-1 cells (10 mice/each group). **a** Tumor volumes over the time course of the experiment ($n = 10$ mice, mean ± s.e.m.). **b** Photographs of tumors from the indicated groups at the end of the study. **c** Tumor weights at study end ($n = 3$–9, mean ± s.e.m.). **d** Human $CD3^+$ T-cell percentages in peripheral blood over the study time course ($n = 10$ mice, mean ± s.e.m.). *$p < 0.05$, **$p < 0.01$, *ns* means not significant

expression patterns in monocytic AML cells.[1,12] Second, LILRB1, LILRB2, and LILRB3 share certain identical AA sequences in their ITIMs.[1] Therefore, we used LILRB1 as a representative LILRB to compare with LILRB4.

lilrb4-WT but not *lilrb4*-KO AML cells were capable of significantly inhibiting T-cell proliferation; knockout of *lilrb1* did not alter the T-cell inhibition ability of AML cells (Fig. 6c, d, Supplementary Figs. S7 and S8). Interestingly, forced expression of the protein with the ECD of LILRB4 and the ID of LILRB1 did not rescue T-cell suppression, whereas T-cell proliferation was significantly inhibited in *lilrb1*-KO cells when the protein with the ECD of LILRB1 and the ID of LILRB4 was expressed (Fig. 6c, d, Supplementary Figs. S7 and S8). The same result was obtained with a histidine-tagged (as the sorting marker for infected cells) version of this protein (Fig. 6a, b, Supplementary Figs. S7 and S8). These results suggest that the ID of LILRB4 has a unique ability to inhibit T-cell proliferation.

LILRB4 supports the infiltration of AML cells into tissues and organs.[12] Whereas *lilrb4*-KO cells expressing the histidine-tagged protein with the ECD of LILRB1 and the ID of LILRB4 significantly enhanced the infiltration of *lilrb4*-KO cells, the expression of the chimera with the ID of LILRB1 did not promote *trans*-endothelial migration (Fig. 7a). Expression of the protein with the ECD of LILRB1 and the ID of LILRB4 in *lilrb1*-KO cells did not significantly promote the *trans*-endothelial migration ability of THP-1 cells (Fig. 7a). There is more robust endogenous LILRB4 signaling in THP-1 cells than signaling from other LILRBs (Fig. 1a), which may make the effects of ectopic expression undetectable in THP-1 cells.

Next, we analyzed the expression of downstream signaling molecules of LILRB4. Compared with that in *lilrb4*-WT cells, the phospho-SHP-2 (Y_{580}) level was decreased in *lilrb4*-KO but not *lilrb1*-KO cells, consistent with a previous report that LILRB1 recruits SHP-1 but not SHP-2.[30] The phospho-SHP-2 (Y_{580}) level was increased in *lilrb4*-KO cells when the chimeric protein with the LILRB4 intracellular domain (His-Tag-B1-ECD-B4-ID) was ectopically expressed, whereas expression of the chimeric protein with the LILRB1 intracellular domain did not increase phospho-SHP-2 (Y_{580}) levels (Fig. 7b and Supplementary Fig. S9A). The phospho-P65 (S_{536}), ARG1, and uPAR levels were also increased by the expression of only the protein with the LILRB4 intracellular domain (Fig. 7b, c and Supplementary Figs. S9B-D). Similar results were observed for F-actin (Fig. 7d and Supplementary Fig. S9E). Together, these results show that the intracellular domain of LILRB4 has a unique function in T-cell inhibition and infiltration by AML cells.

DISCUSSION

We previously demonstrated that LILRB4 supports tumor cell infiltration into tissues and suppresses T-cell activity via the ApoE/LILRB4/SHP-2/uPAR/arginase-1 signaling axis in AML cells.[12] In this study, we focused on two questions: what ITIMs of LILRB4 are required for inhibiting T-cell proliferation and promoting infiltration of monocytic AML cells, and do the intracellular domains of another LILRB family member have similar signaling functions to those of LILRB4 in leukemia cells.

We found that the second (Y_{412}) and the third (Y_{442}) ITIMs of LILRB4, but not the first (Y_{360}), are required for LILRB4-mediated signaling and for the inhibition of T-cell proliferation induced by monocytic AML cells (Fig. 8). Therefore, the two functions of LILRB4 in monocytic AML cells, T-cell inhibition and infiltration, depend on slightly different ITIMs and perhaps on different signaling effectors. The fact that the ITIMs in LILRB4 have different functions is in accordance with a recent report on the roles of LILRB4 ITIMs in monocyte functions, including TNFα production and bactericidal activity.[25] Both studies support the conclusion that the effects of LILRB4 ITIMs are related to context- and function-dependent differences in downstream signaling.

We also investigated whether the intracellular domain of LILRB1 has a similar function to that of LILRB4 in AML cells. Although both contain ITIMs, the intracellular domain of LILRB1 does not support the two functions of LILRB4 in AML cells. There are several possible

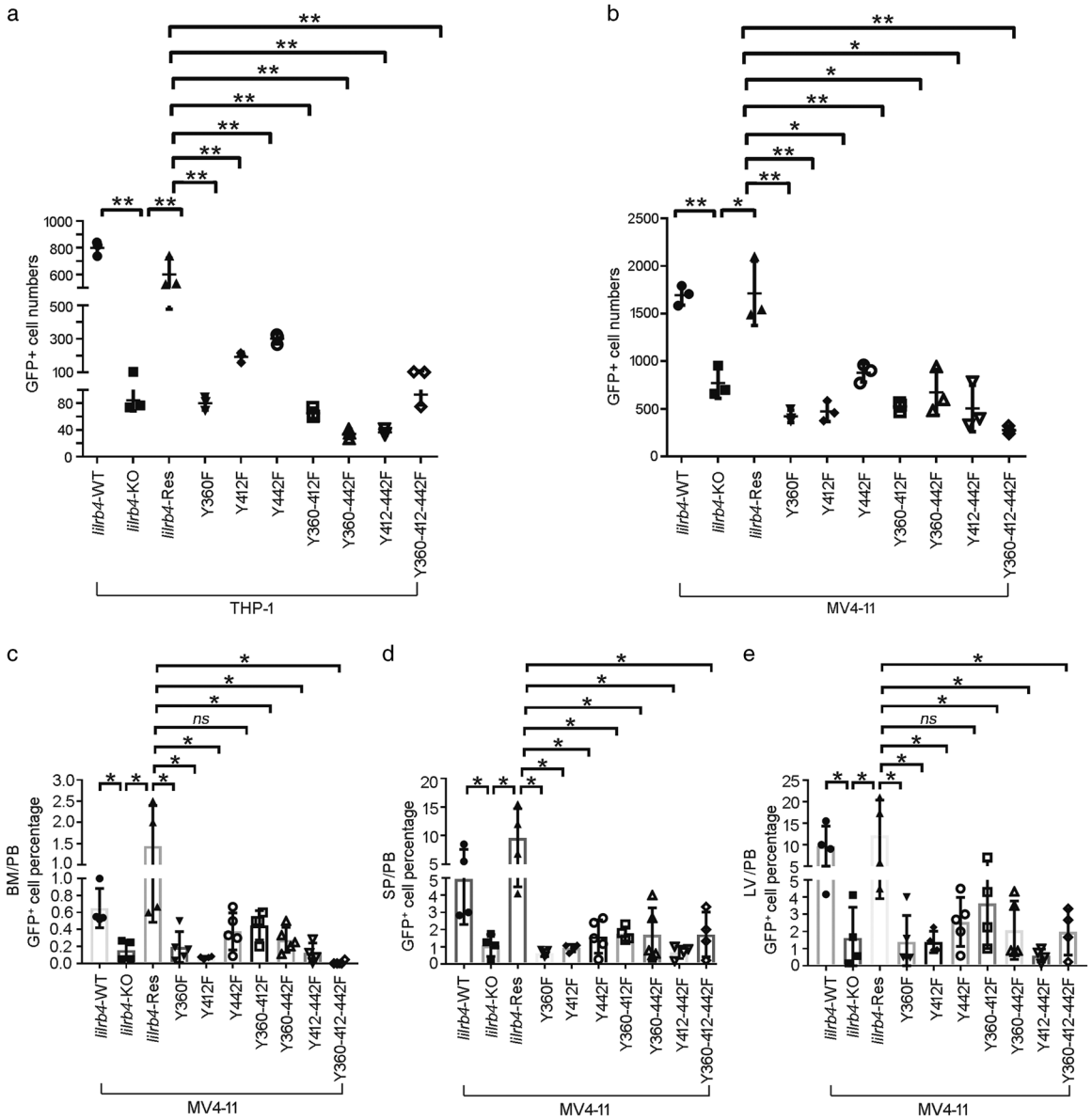

Fig. 3 Y_{360}, Y_{412}, and Y_{442} of LILRB4 are necessary for the infiltration of monocytic AML cells in vitro and in vivo. **a**, **b** *Trans*-endothelial migration of (**a**) THP-1 or (**b**) MV4-11 cells was quantified by counting the GFP^+ cells isolated by flow cytometry ($n = 3$, mean ± s.e.m.). **c**–**e** MV4-11 cells were injected into NSG mice ($n = 4$–5 mice, mean ± s.e.m.). After 20 h, GFP^+ cell percentages in (**c**) bone marrow (BM), (**d**) spleen (SP), and (**e**) liver (LV) were determined. Numbers were normalized to GFP^+ cell percentages in peripheral blood (PB). *$p < 0.05$, **$p < 0.01$, *ns* means not significant

reasons for this very unusual observation. First, it is possible that different signaling molecules (in addition to SHP-1 and SHP-2) can be recruited by different LILRB family members. LILRB1 contains four ITIMs.[30] Y_{533} (NLYAAV) is needed for tyrosine phosphorylation and subsequent SHP-1 recruitment, whereas Y_{644} (SIYATL) and Y_{614} (VTYAQL) act as the SHP-1 docking sites.[30] Y_{562} (VTYAEV) does not have an SHP-1-related signaling function.[30] It has been suggested that Y_{562} is the main docking site for the Src kinase CSK and that Y_{533} and Y_{614} contribute to CSK binding; however, SHP-1 and CSK do not exist in the same LILRB1 complex.[30] PirB, a mouse orthologue of the LILRB family proteins, can interact with SHP-1, SHP-2, Btk, Src, Syk, and Yes, and PirB may recruit Hck to regulate noninhibitory signaling pathways.[29,31] Based on these observations, it is possible that unique signaling molecules interact with each LILRB. Second, the net outcome of LILRB signaling can be regulated by other signaling pathways. For example, PirB signaling can be enhanced by TLR9 signaling activation,[5] and after LTB4-induced activation, PirB can interact with kinases such as JAK1, JAK2, Shc, and Crk.[27,31] It is therefore possible that LILRB1 and LILRB4 respond differently to other pathways in AML cells. Third, although ITIMs are the only identified signaling motifs in LILRBs, additional motifs in LILRB1 or LILRB4 may work cooperatively with ITIMs. For example, the unique proline-rich motif of LILRB4 has the potential to interact with SH3-domain molecules.[32]

It has been shown that LILRB4 levels on dendritic cells are upregulated by Tregs.[33,34] It will be important to know whether membrane-bound protein–protein interactions or soluble factor(s) mediate this effect. Although it has been reported that the interaction of LILRB4 with CD166 mediates its inhibitory effect on tumor cells,[35] and we demonstrated that ApoE can activate LILRB4, further investigations are needed to clarify whether LILRB4 on monocytic cells (including dendritic cells) can directly bind and act on a surface protein (ideally an immune inhibitory receptor) on activated or regulatory T cells.

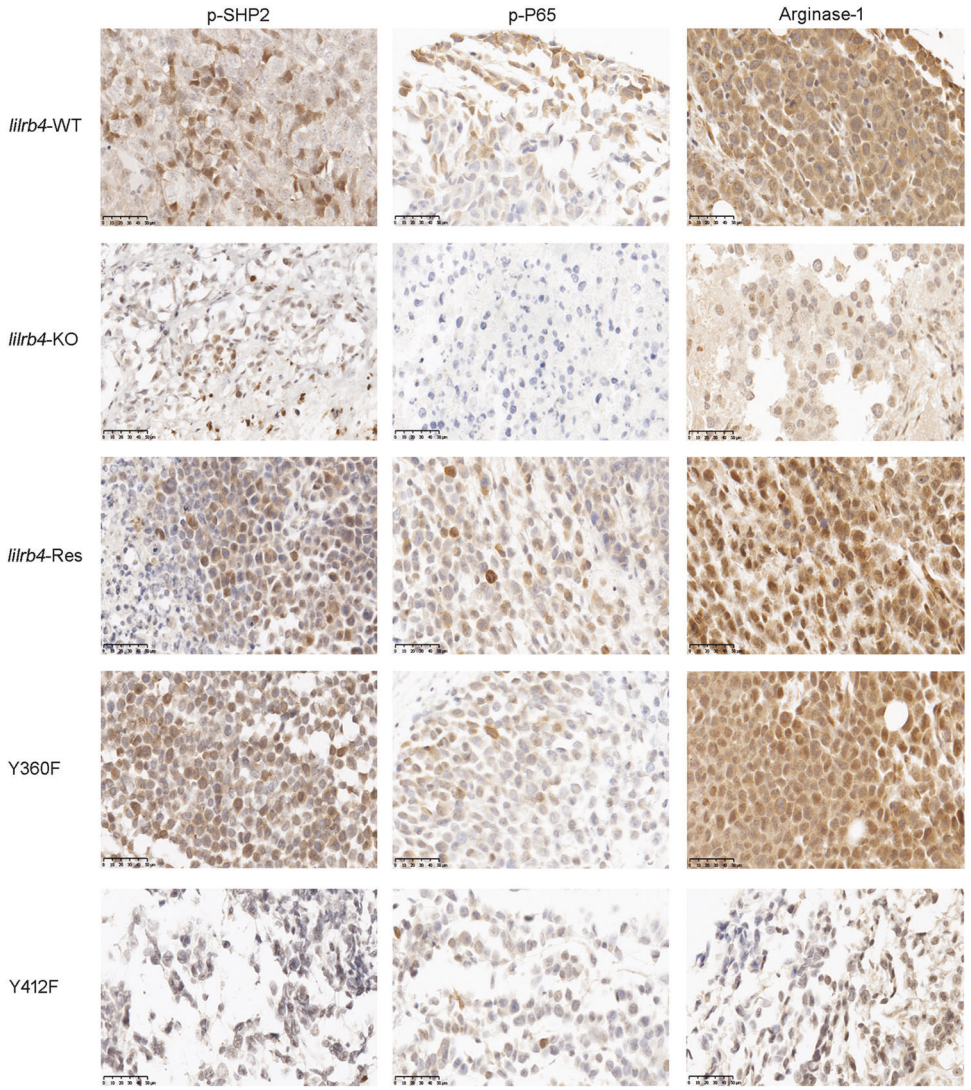

Fig. 4 Detection of LILRB4 downstream signaling molecules in human T cell reconstituted xenograft samples by immunohistochemistry. Tumor sections from NSG mice transplanted with 1×10^7 *lilrb4*-WT, *lilrb4*-KO, *lilrb4*-Res, *lilrb4*-$Y_{360}F$, *lilrb4*-$Y_{412}F$, or *lilrb4*-$Y_{442}F$ THP-1 cells were stained with antibodies against phospho-SHP-2 (Y_{580}), phospho-P65, and arginase-1. The scale bars are 50 μm

In summary, we have defined the signaling roles of the ITIMs of LILRB4 in the inhibition of T-cell activity and the migration of AML cells. Our elucidation of the functions of the three ITIMs of LILRB4 in monocytic AML cells deepens our understanding of the mechanism by which this receptor regulates immune checkpoints and tumor development. These findings may also facilitate the engineering of ITIMs for the development of novel cell therapies.

MATERIALS AND METHODS

Cells

Human cell lines were purchased from ATCC. THP-1 and MV4-11 cells were cultured in RPMI-1640 medium (Sigma-Aldrich, R8758) with 10% heat-inactivated fetal bovine serum (FBS, Sigma-Aldrich, F2442) and 1% penicillin and streptomycin (P4333, Sigma-Aldrich). Human umbilical vascular endothelial cells (hUVECs) were cultured in an endothelial culture medium kit (EGM-BulletKit, Lonza). 293T cells were cultured in Dulbecco's modified Eagle's medium/high glucose (Sigma-Aldrich, D5796) with 10% heat-inactivated fetal bovine serum and 1% penicillin and streptomycin. All cells were incubated at 37 °C in a 5% CO_2 incubator.

Mice

Immune compromised NOD-scid *IL2Rγ*-knockout (NSG) mice were purchased from the animal core facility of the University of Texas Southwestern Medical Center (UTSW). All animal experiments were performed with the approval of the UT Southwestern Institutional Animal Care and Use Committee.

lilrb4- and *lilrb1*-knockout lines

lilrb4 and *lilrb1* were knocked out using the CRISPR-Cas9 system as described previously.[12] The sgRNA sequences were designed at http://crispr.mit.edu, and the sequences were as follows:

control sgRNA: 5′-GAACGACTAGTTAGGCGTGTA-3′

sgRNAs targeting *lilrb4*:

sgRNA1: 5′-TGTTACTATCGCAGCCCTGT-3′;

sgRNA2: 5′-GTAGGTCCCCCCGTGCACTG-3′;

sgRNA3: 5′-CCTGTGACCTCAGTGCACGG-3′

sgRNAs targeting *lilrb1*:

sgRNA1: 5′-TACTATGGTAGCGACACTGC-3′

sgRNA2: 5′-TCCCTCCTGAGTTCACCACG-3′

These sequences were subcloned into a sgRNA expression plasmid followed by introduction into cells by lentiviral

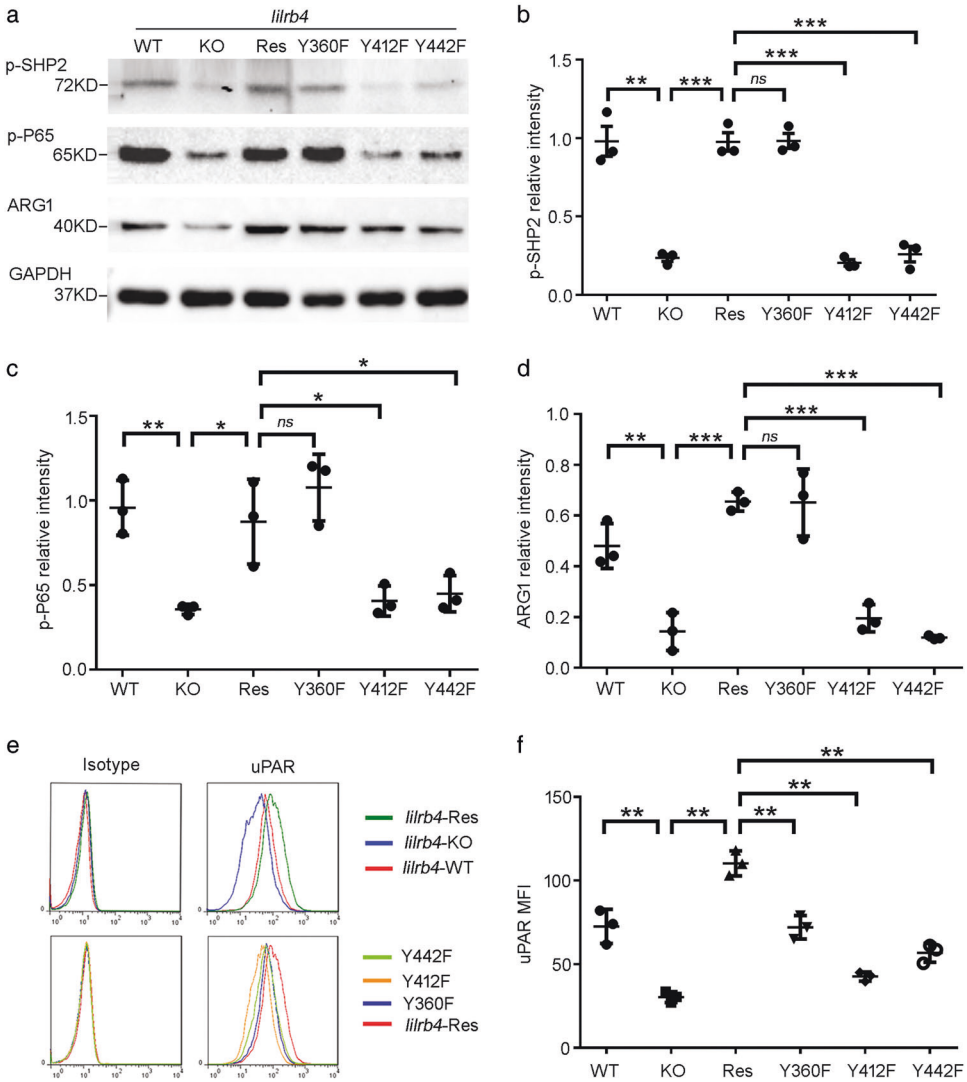

Fig. 5 Y_{412} and Y_{442} but not Y_{360} regulate uPAR and ARG1 status. Phospho-SHP-2 and phospho-P65 ARG1 were detected by western blotting (**a**), and uPAR was measured by flow cytometry (**d**). Their levels were quantified from three independent experiments (**b**–**d**, **f**). Representative data from three independent experiments are presented ($n = 3$, means ± s.e.m.). MFI: mean fluorescence intensity, $^{**}p < 0.01$, $^{***}p < 0.001$, *ns* means not significant

transduction. After 1 μg/ml doxycycline induction for 7 days, cells were stained with APC-conjugated mouse anti-human LILRB4 (eBioscience, 17-5139-41, 1:200) or APC-conjugated mouse anti-human LILRB1 (eBioscience, 17-5129-41, 1:200), and GFP-positive and LILRB4- or LILRB1-negative cells were selected using a BD FACSAria.

Chimeric plasmids and position-directed mutagenesis

The chimeric plasmids for expression of the extracellular domain (ECD) of LILRB4 fused with the transmembrane and intracellular domain (ID) of LILRB1 (B4-ECD-B1-ID), for the expression of the ECD of LILRB1 fused with the transmembrane and intracellular domain of LILRB4 (B1-ECD-B4-ID) and for the expression of histidine-tagged His-Tag-B1-ECD-B4-ID were constructed by overlapping PCR. The sequences of the primers are given below. The underlining indicates the In-Fusion sequences, and italics represent the overlapping sequences.

lilrb4-*ECD*. F: 5′-ATCTATTTCCGGTGAATTCCATGATCCCCACCTTCACG-3′
R: 5′-***GTGATCGGCA***CTCCCAGTGC-3′

lilrb4-*ID*. F: 5′-GTACTGATCGGGGTCTTG-3′
R: 5′-GGGCGGGATCCGCGGCCGCTTTAGTGGATGGCCAGAGTG-3′

lilrb1-*ECD*. F: 5′-ATCTATTTCCGGTGAATTCCATGACCCCCATCCTCACG-3′
R: 5′-***GTACTGATCG***AACCCCCAGG-3′

lilrb1-*ID*. F: 5′-GTGATCGGCATCTTGGTG-3′
R: 5′-GGGCGGGATCCGCGGCCGCTCTAGTGGATGGCCAGAGTG-3′

His-Tag-B1-ECD-B4-ID. F: 5′-TCACCATCATGGAGGCTCTGGGGCACCTCCCCAAGCCC-3′
R: 5′-AGAGGGGCGGGATCGCGGCCGCTTTAGTGGATGGCCAGAGTGGCATAG-3′

PCR fragments were amplified and cloned into the pLVX-IRES-ZsGreen vector using the InFusion kit (Takara Bio). Three single mutants ($Y_{360}F$, $Y_{412}F$, and $Y_{442}F$), three double mutants ($Y_{360–412}F$, $Y_{360–442}F$, and $Y_{412–442}F$), and one triple mutant ($Y_{360–412–442}F$) were constructed using the following primers. The italics indicate the sites of mutations. Because the Y442 site is close to the C terminus of LILRB4, the tyrosine codon (TAT) was mutated to

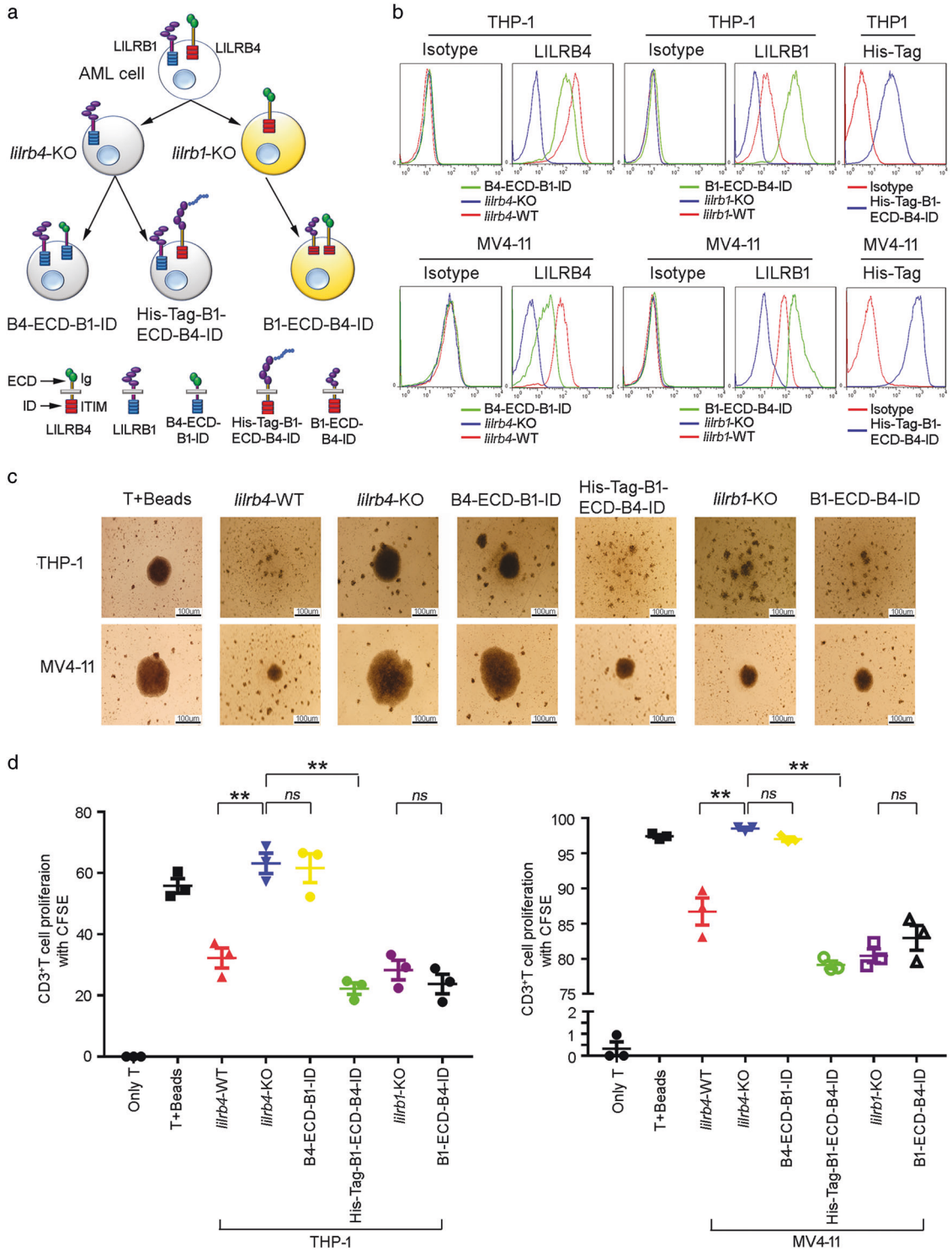

Fig. 6 The intracellular domain of LILRB4, but not that of LILRB1, mediates T-cell inhibition by AML cells. **a**, **b** Vectors for expression of B4-ECD-B1-ID, His-Tag-B1-ECD-B4-ID, and B1-ECD-B4-ID were constructed by swapping the regions encoding the ECDs of *lilrb4* and *lilrb1*, and proteins were expressed in *lilrb4*-KO or *lilrb1*-KO cells. Expression was evaluated by FACS. **c**, **d** Human $CD3^+$ T cells were cocultured with AML cells expressing chimeric proteins. **c** $CD3^+$ T-cell cultures were photographed after 5 days (scale bar: 100 μm), and **d** T-cell proliferation was quantified by CFSE dilution detected by flow cytometry ($n = 3$, means ± s.e.m.). Representative data from three independent experiments are presented. $^{**}p < 0.01$, *ns* means not significant

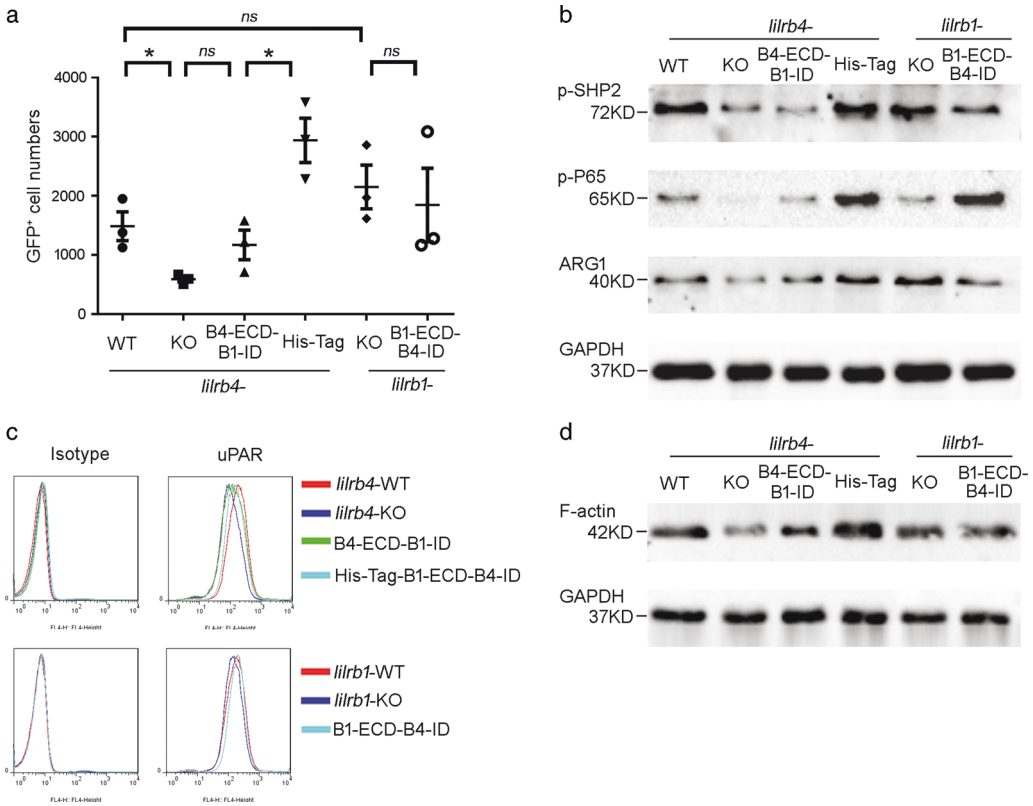

Fig. 7 The intracellular domain of LILRB4, but not that of LILRB1, promotes the *trans*-endothelial migration of AML cells. **a** *Trans*-endothelial migration of GFP$^+$ THP-1 cells was quantified by flow cytometry ($n = 3$, means ± s.e.m.). **b**–**d** The downstream signaling molecules of LILRB4 were detected in *lilrb4*-KO or *lilrb1*-KO THP-1 cells expressing the indicated chimeric vectors. Phospho-SHP-2, phospho-P65, ARG1, and F-actin were detected by Western blotting (**b**, **d**), and uPAR was measured by flow cytometry (**c**). Representative data from three independent experiments are presented. His-Tag means His-Tag-B1-ECD-B4-ID, $*p < 0.05$, *ns* means not significant

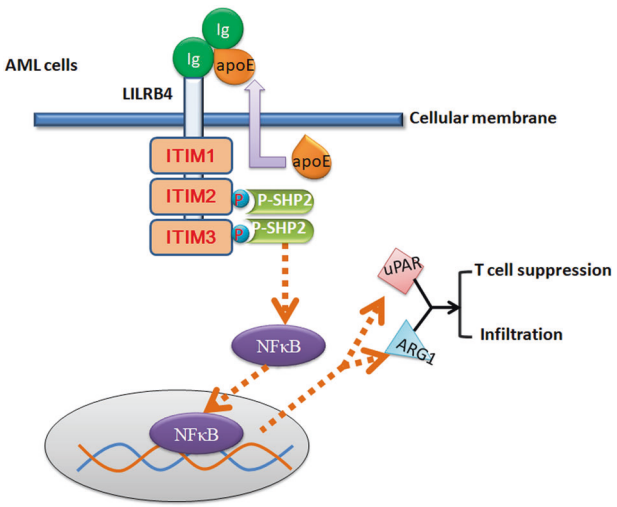

Fig. 8 Schematic for the mechanisms by which LILRB4 ITIMs inhibit T-cell proliferation and promote AML infiltration and migration

phenylalanine (AAA) in only the reverse primer, and the forward primer amplifying the full-length CDS of *lilrb4* was used to amplify the *lilrb4*-Y442F fragment.

$Y_{360}F$. F: 5′-GCAGTGACG*TTC*GCCAAGGTGAAACACTCCAGAC-3′
R: 5′-GTCTGGAGTGTTTCACCTTGGCG*AA*CGTCACTGC-3′

$Y_{412}F$. F: 5′-GGATGTGACC*TTC*GCCCAGCTGCACAG-3′
R: 5′-CTGTGCAGCTGGGC*GAA*GGTCACATCC-3′

$Y_{442}F$. F: 5′-ATCTATTTCCGGTGAATTCCATGATCCCCACCTTCACG-3′
R: 5′-TTAATTCTAGATTAGTGGATGGCCAGAGTGGC*AAA*GA-3′
The desired fusions and mutations were confirmed by sequencing.

Lentivirus packaging and infection

The desired CRISPR-Cas9-based sgRNA vector or pLVX-IRES-ZsGreen-*hlilrb4*, pLVX-IRES-ZsGreen-B1-ECD-B4-ID, pLVX-IRES-ZsGreen-B4-ECD-B1-ID, pLVX-IRES-ZsGreen-His-Tag-B1-ECD-B4-ID, pLVX-IRES-ZsGreen-$Y_{360}F$, pLVX-IRES-ZsGreen-$Y_{412}F$, pLVX-IRES-ZsGreen-$Y_{442}F$, pLVX-IRES-ZsGreen-$Y_{360-412}F$, pLVX-IRES-ZsGreen-$Y_{360-442}F$, pLVX-IRES-ZsGreen-$Y_{412-442}F$, or pLVX-IRES-ZsGreen-$Y_{360-412-442}F$ vectors were mixed with psPAX2 and pMD2.G at a ratio of 4:3:1 and transfected into 293T cells using PolyJet Reagent (Signagen). After 48 and 72 h, virus-containing supernatants were collected for infection as previously described.[12]

Leukemia cell and T-cell coculture assay

As described previously,[12] we used the permeable support system (pore size 3.0 μm, Fisher Clontech) for the leukemia cell and T-cell coculture in U-bottom 96-well plates. We placed 5×10^4 human CD3$^+$ T cells (all cells) isolated from the healthy donor peripheral blood into the lower chamber and irradiated THP-1 or MV4-11 cells (2.5×10^4 per well, 28 Gy) into the transwell upper chamber. T cells were labeled with CFSE (CellTrace CFSE Cell Proliferation Kit, Thermo Fisher Scientific). IL-2 (50 U/ml, Novoprotein) and Dynabeads Human T-activator CD3/CD28 (Thermo Fisher Scientific,

25 μl/1 × 10^6 cells) were added to complete RPMI-1640 medium. After 5–7 days, T cells were stained with APC-conjugated-mouse-anti-human CD3 (BioLegend, 317318) and PE-conjugated-mouse-anti-human CD8 (BD Pharmingen, 555367). T-cell proliferation was analyzed by CFSE dilution. Unstimulated T cells were used as negative controls, and Dynabeads without stimulated cells served as positive controls.

Flow cytometry

Primary antibodies, including anti-human LILRB4-APC (eBioscience, ZM4.1, 1:200), anti-human LILRB1-APC (eBioscience, HP-F1, 1:200), anti-human CD3-APC (BioLegend, OKT3, 1:200), anti-human CD8-PE (BD Pharmingen, 555367, 1:200), anti-His-Tag-PE (BioLegend, 362603, 1:100), and anti-human uPAR-APC (BioLegend, VIM5, 1:100), were used. Samples from NSG mice were analyzed as described previously.[12]

Trans-endothelial migration assays

hUVECs were cultured at 3 × 10^5 cells per chamber in 24-well transwell upper chambers (8.0 μm, Fisher). After 3 days, 1 × 10^5 THP-1 or MV4-11 cells were added to the upper chamber. After 20 h, the medium was collected from the lower chamber, and GFP^+ cells were counted by flow cytometry to observe *trans*-endothelial migration.[12]

Short-term infiltration assay

For analysis of infiltration in vivo, 3 × 10^6 MV4-11 cells were intravenously transplanted into 6–8-week-old NSG mice by tail veil injection. After 20 h, peripheral blood was taken under anesthesia, and the mice were sacrificed. The spleen, liver, and bone marrow were collected, dissected by scissors, and filtered through 300 μm mesh filters to make single-cell suspensions. The number of GFP^+ cells was determined by flow cytometry with normalization to the cell numbers in peripheral blood.

Xenograft model in humanized mice

As described previously,[12] fresh human peripheral blood mononuclear cells (PBMCs) were isolated from the buffy coat (Interstate Blood Bank, Memphis, TN) by Ficoll Hypaque density gradient separation (GE Lifesciences), and the red blood cells were removed by lysis. Each NSG mouse was given 1 × 10^7 human PBMCs by intraperitoneal injection. After 7 days, human $CD3^+$ T cells were detected in peripheral blood by flow cytometry. Mice (10 mice/each group) were grouped according to the $CD3^+$ T-cell levels, and 1 × 10^7 THP-1 *lilrb4*-wild-type (WT), *lilrb4*-knockout (KO), *lilrb4*-rescue (Res), *lilrb4*-Y_{360}F, *lilrb4*-Y_{412}F, or *lilrb4*-Y_{442}F cells were subcutaneously implanted. The tumor sizes were measured every 5 days, and the T-cell percentage in peripheral blood was detected every 7 days. The mice were sacrificed under anesthesia when moribund. The tumor, spleen, bone marrow, and liver were isolated, and the human $CD3^+$ T-cell percentage was detected by flow cytometry.

Western blotting

As described previously,[12] equal amounts of protein were separated by SDS-PAGE and then transferred to a nitrocellulose membrane. The primary antibodies used were anti-phospho-SHP-2 (Tyr_{580}, Cell Signaling Technology, 13328S, 1:500), anti-phospho-p65 (Ser_{536}, Cell Signaling Technology, 3033T, 1:1000), anti-arginase-1 (Cell Signaling Technology, 9819, 1:1000), anti-F-actin (Bioss, bs-1571R, 1:500), and anti-GAPDH (Cell Signaling Technology, 5174, 1:1000). Membranes were incubated with antibody overnight at 4 °C.

Coimmunoprecipitation

Cells were collected and lysed by IP lysis buffer (0.025 M Tris, 0.15 M NaCl, 0.001 M EDTA, 1% NP-40, and 5% glycerol; pH = 7.4) with a protease inhibitor cocktail (Roche Diagnostics). The samples were incubated with anti-LILRB4 antibody overnight at 4 °C. The magnetic beads (Invitrogen, 10003D) were added and incubated for 15 min at room temperature. The magnetic bead-Ab-Ag complex was washed 5 times, and the samples were separated by SDS-PAGE. Anti-SHP-2 (Cell Signaling Technology, 3397, 1:500) was incubated with the samples overnight at 4 °C.

Immunohistochemistry

Paraffin-embedded tumor samples were treated as detailed in our previous reports.[12] Antibodies against phospho-SHP-2 (Y_{580}, Cell Signaling Technology, 13328S, 1:200), phospho-P65 (S_{536}, Cell Signaling Technology, 3033T, 1:200), and arginase-1 (Cell Signaling Technology, 9819, 1:200) were used for staining. Samples were scanned using a Hamamatsu NanoZoomer 2.0-HT (Meyer Instruments).

Statistical analysis

Representative data from three independent experiments or the indicated number of independent samples are presented, and statistical significance for two-sample comparisons was calculated by ANOVA. $p < 0.05$ was considered statistically significant.

ACKNOWLEDGEMENTS

We thank the National Cancer Institute (1R01CA172268), the Cancer Prevention and Research Institute of Texas (RP180435), the Robert A. Welch Foundation (I-1834), China Natural Science Foundation (81872332), Shandong Natural Science Foundation (2018GSF118201), and Yantai Science and Technology Development Plan (2018ZHGY070) for generous support.

AUTHOR CONTRIBUTIONS

ZL.L., M.D., and CC.Z. designed the study and wrote the paper. ZL.L., M.D., FF.H., HY.C., XY.L., and LC.H. performed the mouse experiments. ZL.L., FF.H., CZ.J., and S.S. performed the flow cytometry analysis and western blotting. ZL.L., M.D., HY.C., XY.L., and AH.S. performed the CRISPR-Cas9 experiments and plasmid constructions. ZL.L. and M.D. performed the T-cell coculture and IHC. ZL.L., and M.D. performed the statistical analysis.

ADDITIONAL INFORMATION

The online version of this article (https://doi.org/10.1038/s41423-019-0321-2) contains supplementary material.

Competing interests: C.C.Z. is a scientific founder of Immune-Onc Therapeutics. C.C.Z. and M.D. hold equity in and have multiple patents licensed to Immune-Onc Therapeutics. The other authors declare no competing interests.

REFERENCES

1. Kang, X. et al. Inhibitory leukocyte immunoglobulin-like receptors: immune checkpoint proteins and tumor sustaining factors. *Cell Cycle* **15**, 25–40 (2016).
2. Hirayasu, K. & Arase, H. Functional and genetic diversity of leukocyte immunoglobulin-like receptor and implication for disease associations. *J. Hum. Genet.* **60**, 703–708 (2015).
3. Trowsdale, J., Jones, D. C., Barrow, A. D. & Traherne, J. A. Surveillance of cell and tissue perturbation by receptors in the LRC. *Immunol. Rev.* **267**, 117–136 (2015).
4. Daeron, M., Jaeger, S., Du Pasquier, L. & Vivier, E. Immunoreceptor tyrosine-based inhibition motifs: a quest in the past and future. *Immunol. Rev.* **224**, 11–43 (2008).
5. Takai, T., Nakamura, A. & Endo, S. Role of PIR-B in autoimmune glomerulonephritis. *J. Biomed. Biotechnol.* **2011**, 275302 (2011).
6. Katz, H. R. Inhibition of inflammatory responses by leukocyte Ig-like receptors. *Adv. Immunol.* **91**, 251–272 (2006).
7. Carosella, E. D., Rouas-Freiss, N., Roux, D. T., Moreau, P. & LeMaoult, J. HLA-G: an Immune Checkpoint Molecule. *Adv. Immunol.* **127**, 33–144 (2015).
8. Colovai, A. I. et al. Expression of inhibitory receptor ILT3 on neoplastic B cells is associated with lymphoid tissue involvement in chronic lymphocytic leukemia. *Cytom. Part B, Clin. Cytom.* **72**, 354–362 (2007).
9. Zurli, V. et al. Ectopic ILT3 controls BCR-dependent activation of Akt in B-cell chronic lymphocytic leukemia. *Blood* **130**, 2006–2017 (2017).

10. Zheng, J. et al. Inhibitory receptors bind ANGPTLs and support blood stem cells and leukaemia development. *Nature* **485**, 656–660 (2012).
11. Kang, X. et al. The ITIM-containing receptor LAIR1 is essential for acute myeloid leukaemia development. *Nat. Cell Biol.* **17**, 665–677 (2015).
12. Deng, M. et al. LILRB4 signalling in leukaemia cells mediates T cell suppression and tumour infiltration. *Nature* **562**, 605–609 (2018).
13. John, S. et al. A novel anti-LILRB4 CAR-T cell for the treatment of monocytic AML. *Mol. Ther.* **26**, 2487–2495 (2018).
14. Suciu-Foca, N. et al. Soluble Ig-like transcript 3 inhibits tumor allograft rejection in humanized SCID mice and T cell responses in cancer patients. *J. Immunol.* **178**, 7432–7441 (2007).
15. Barkal, A. A. et al. Engagement of MHC class I by the inhibitory receptor LILRB1 suppresses macrophages and is a target of cancer immunotherapy. *Nat. Immunol.* **19**, 76–84 (2018).
16. Chen, Z. et al. Signalling thresholds and negative B-cell selection in acute lymphoblastic leukaemia. *Nature* **521**, 357–361 (2015).
17. Perna, F. et al. Integrating proteomics and transcriptomics for systematic combinatorial chimeric antigen receptor therapy of AML. *Cancer Cell* **32**, 506–519 e505 (2017).
18. Cella, M. et al. A novel inhibitory receptor (ILT3) expressed on monocytes, macrophages, and dendritic cells involved in antigen processing. *J. Exp. Med.* **185**, 1743–1751 (1997).
19. Inui, M. et al. Human CD43+ B cells are closely related not only to memory B cells phenotypically but also to plasmablasts developmentally in healthy individuals. *Int Immunol.* **27**, 345–355 (2015).
20. Dobrowolska, H., Vlad, G. & Suciu-Foca, N. Expression of inhibitory receptor ILT3 on normal hematopoietic stem cells and leukemic progenitors. *J. Cell Sci. Ther.* **4**, 98 (2013).
21. Dobrowolska, H. et al. Expression of immune inhibitory receptor ILT3 in acute myeloid leukemia with monocytic differentiation. *Cytom. Part B, Clin. Cytom.* **84**, 21–29 (2013).
22. Gui, X. et al. Disrupting LILRB4/APOE interaction by an efficacious humanized antibody reverses T-cell suppression and blocks AML development. *Cancer Immunol. Res.* **7**, 1244–1257 (2019).
23. Baitsch, D. et al. Apolipoprotein E induces antiinflammatory phenotype in macrophages. *Arteriosclerosis, Thrombosis, Vasc. Biol.* **31**, 1160–1168 (2011).
24. Samaridis, J. & Colonna, M. Cloning of novel immunoglobulin superfamily receptors expressed on human myeloid and lymphoid cells: structural evidence for new stimulatory and inhibitory pathways. *Eur. J. Immunol.* **27**, 660–665 (1997).
25. Park, M. et al. A dual positive and negative regulation of monocyte activation by leukocyte Ig-like receptor B4 depends on the position of the tyrosine residues in its ITIMs. *Innate Immun.* **23**, 381–391 (2017).
26. Ishige, M. et al. A case of metastatic spermatic cord tumor from acute myelogenous leukemia. *Nihon Hinyokika Gakkai zasshi Jpn. J. Urol.* **103**, 631–635 (2012).
27. Straus, D. J. et al. The acute monocytic leukemias: multidisciplinary studies in 45 patients. *Medicine* **59**, 409–425 (1980).
28. Wang, Y. et al. Identification of a novel nuclear factor-kappaB sequence involved in expression of urokinase-type plasminogen activator receptor. *Eur. J. Biochem.* **267**, 3248–3254 (2000).
29. Zhang, H., Meng, F., Chu, C. L., Takai, T. & Lowell, C. A. The Src family kinases Hck and Fgr negatively regulate neutrophil and dendritic cell chemokine signaling via PIR-B. *Immunity* **22**, 235–246 (2005).
30. Bellon, T., Kitzig, F., Sayos, J. & Lopez-Botet, M. Mutational analysis of immunoreceptor tyrosine-based inhibition motifs of the Ig-like transcript 2 (CD85j) leukocyte receptor. *J. Immunol.* **168**, 3351–3359 (2002).
31. Munitz, A., McBride, M. L., Bernstein, J. S. & Rothenberg, M. E. A dual activation and inhibition role for the paired immunoglobulin-like receptor B in eosinophils. *Blood* **111**, 5694–5703 (2008).
32. Lu-Kuo, J. M., Joyal, D. M., Austen, K. F. & Katz, H. R. gp49B1 inhibits IgE-initiated mast cell activation through both immunoreceptor tyrosine-based inhibitory motifs, recruitment of src homology 2 domain-containing phosphatase-1, and suppression of early and late calcium mobilization. *J. Biol. Chem.* **274**, 5791–5796 (1999).
33. Chang, C. C. et al. Tolerization of dendritic cells by T(S) cells: the crucial role of inhibitory receptors ILT3 and ILT4. *Nat. Immunol.* **3**, 237–243 (2002).
34. Cousens, L., Najafian, N., Martin, W. D. & De Groot, A. S. Tregitope: immunomodulation powerhouse. *Hum. Immunol.* **75**, 1139–1146 (2014).
35. Xu, Z. et al. ILT3.Fc-CD166 interaction induces inactivation of p70 S6 kinase and inhibits tumor cell growth. *J. Immunol.* **200**, 1207–1219 (2018).